

## An Investigation on Structural, Electrical and Optical properties of GO/ZnO Nanocomposite

Virginia Mututu, Sunitha A K, Riya Thomas, Mayank Pandey, Manoj B\*

Department of Physics & Electronics, CHRIST (Deemed to be University), Bengaluru, Karnataka, India

\*E-mail: [manoj.b@christuniversity.in](mailto:manoj.b@christuniversity.in)

Received: 28 August 2018/ Accepted: 20 October 2018 / Published: 10 March 2019

---

Coupling of graphene oxide with metal oxide is an effective way to enhance the opto-electric properties of the composite. Herein, a hybrid structure of graphene oxide (GO) –Zinc oxide (ZnO) nanostructure was successfully designed and fabricated with varying concentrations of ZnO. The GO and ZnO nanoparticles were synthesized through Hummer's and simple precipitation method respectively. Structural and physiochemical properties were examined via X-ray powder diffraction, FTIR and UV-Vis spectroscopy. The XRD results of GO showed a peak at  $2\theta$  of  $12.02^\circ$  with particles of size 6nm and inter layer spacing 0.87 nm. The XRD patterns of ZnO nanoparticles showed a hexagonal unit cell structure and the average dimension of the sample was calculated to be 15 nm. The band gap of the synthesized GO is found to be 5.1 eV and that of ZnO to be 3.07 eV with the help Tauc plot. The dependence of various concentration of ZnO on the electrical behaviour is discussed by an impedance analyzer in the frequency range 100Hz to 1MHz. The ZnO/GO composite with best results have been obtained for 20% and 60 % ratios of ZnO. The composite has high dielectric permittivity and low loss tangent values and is identified as a promising candidate for energy storage applications.

---

**Keywords:** Nanocomposite, Graphene oxide, Tin oxide, physiochemical properties.

### 1. INTRODUCTION

Graphene is a single layered carbon material, of outstanding electrical and mechanical properties. These layered materials have fascinating like exceptional electron-transport, electrical properties and excellent photo catalytic activity [1-2]. Even though graphene and its derivatives have many quoted advantages, its application in semiconductor industry is limited owing to the absence of band gap [3-4]. Graphene and its derivatives when combined with inorganic nanoparticles such as  $\text{TiO}_2$ ,  $\text{SnO}_2$  and ZnO shows enhanced properties like higher efficiency of solar cells, fuel cells and photo catalytic reduction. One can introduce the required band gap in the graphene system by making them dots or by

making graphene-metal oxide composite. It has been reported that the composite of carbon material with polymer/metal oxides or both display higher electrochemical behavior owing to the combined effect of the redox reaction of metal oxide and large surface area and conductivity of graphene. In recent years, graphene-based composites are being surveyed for electro-chemical applications. Even though graphene has got superior properties its effective use is hindered by restacking. This could be prevented by making it as a composite with inorganic materials. Incorporation of ZnO nanostructure within graphene matrix which can significantly enhance the structural and electrical properties of the host graphene.

The most suitable graphene derivative for the ZnO-graphene composite must be synthesized from an abundantly available precursor, due to their scalable production and low-cost. Reduced Graphite has a complex structure and has performed sp<sup>2</sup> carbon domains of variable size in nanometer range. These nano crystallites are linked together in a three dimensional network of covalent bonds with epoxy, carboxyl or esters and non-covalent interactions like hydrogen bonding and  $\pi$ - $\pi$  interactions. These nano islands can be extracted with the aid of a reactive solvent by simple oxidation or reflux [5-6]. Zinc Oxide/Graphene Oxide hybrid structure with varying concentrations of ZnO was successfully synthesized and its structural, electrical and optical properties were investigated.

## 2. MATERIALS AND METHODS

### 2.1. Synthesis of Graphene Oxide (GO)

Graphene oxide was fabricated from graphite powder by means of Hummer's method. 2g of Graphite power, 1g of Sodium nitrate and 46ml of Sulphuric acid were stirred for 15 minutes in an ice bath. 6g of KMnO<sub>4</sub> was added to the solution and allowed to cool for 15min. The stirring of the suspended solution continued for another 1hr along with the addition of 92ml of water. Further dilution was done by 280 ml of warm water. The residual permanganate was then treated with 10 ml of H<sub>2</sub>O<sub>2</sub> (30%) in order to reduce it into soluble manganese ions. In the end the resulting solution is filtered, washed with distilled water, and vacuum dried at 60°C for 24 hours to get GO.

### 2.2. Synthesis of Zinc Oxide (ZnO) Nanostructures

The synthesis of ZnO nanoparticles was done by direct precipitation method using the precursors zinc nitrate and KOH[7]. An aqueous solution (0.2M) of Zinc Nitrate Hexahydrate (Zn (NO<sub>3</sub>)<sub>2</sub>.6H<sub>2</sub>O) was prepared by dissolving 5.95g of Zinc nitrate Hexahydrate crystals in 100ml distilled water. KOH (0.4M) solution was added into the (0.2M) zinc nitrate and stirred vigorously at room temperature till a white suspension is formed. The product was centrifuged at 5000 rpm about 20 minutes and washed repeatedly with distilled water and to finish, washed with absolute alcohol. The sample was then calcinated at 500°C for 3 hr.

The Nano composite of GO-ZnO were made by mixing different ratios of respective compounds. The pellets were prepared using hydraulic press to study the dielectric and ac conductivity of samples.

### 3. RESULTS AND DISCUSSION

#### 3.1. Structural characterization

The X-ray profile of the fabricated products is depicted in Fig.1. The broad peaks of GO validate the semi-crystalline and amorphous nature of GO. It shows a diffraction peak at  $10.1^\circ$  due to the complete oxidation of graphite by chemical oxidation and exfoliation. The increased interlayer spacing  $d=0.874$  nm can attributed to the intercalation of oxygen in the course of oxidation process. The particle size was calculated to be 6 nm using modified Scherrer equation. Thus the results of XRD confirmed the successful synthesis of GO. From the X-ray pattern analysis of ZnO, diffraction peaks located at  $31.74^\circ$ ,  $34.82^\circ$ ,  $36.53^\circ$ ,  $47.53^\circ$ ,  $56.63^\circ$ ,  $63.01^\circ$ ,  $68.23^\circ$ , and  $69.08^\circ$  have indexed as its hexagonal wurtzite phases. The size of the particle was estimated to be 15 nm from the more intense peak at  $36.33^\circ$  corresponding to the 101 plane [8-11]. Absence of any characteristic peak other than ZnO peak confirms the purity of nanopowder.

When GO is made a composite with ZnO (40% and 60%) the two graphitic peaks at  $10^\circ$  and  $26^\circ$  disappears and new peak of ZnO appears in the composite [12] (Fig.1). It is the high crystallinity of ZnO nanoparticles which weakens the GO diffraction peaks. But, ZnO-GO composite as such shows less crystallinity due to the amorphous and nano crystalline structure of GO. Though the intensity of the peaks, reduced with the increase in amount of GO, peak got broadened.

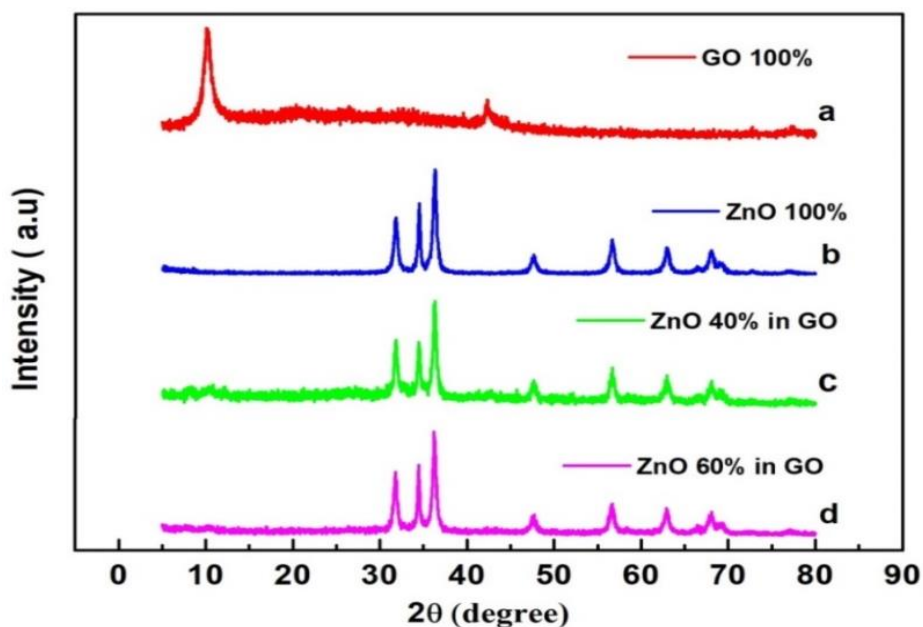


**Figure 1.** XRD pattern of (a) Pure GO (b) Pure ZnO (c) GO-ZnO (60%-40%) (d) GO-ZnO (40%-60%)

FTIR spectra analysis was performed for the structural elucidation and inspection of functional groups in the samples (fig.2). GO showed a broad peak between  $3100-3600\text{cm}^{-1}$  and a sharp peak at  $1626\text{cm}^{-1}$  due to the stretching and bending vibration of OH groups. It concludes the presence of water

molecules adsorbed on GO and strong hydrophilicity of the sample. The absorption peaks in the mid-frequency area at  $2750\text{ cm}^{-1}$  and  $2830\text{ cm}^{-1}$  can be ascribed to the symmetric and anti-symmetric stretching of  $\text{CH}_2$ . The stretching vibration of  $\text{C}=\text{O}$  of carbonyl group,  $\text{C}-\text{O}$  of carboxylic acid and  $\text{C}-\text{OH}$  of alcohol are revealed by the peaks at  $1700\text{ cm}^{-1}$ ,  $1300\text{ cm}^{-1}$  and  $1100\text{ cm}^{-1}$  respectively [13-15]. These oxygen functional groups are created by the oxidation route involved in the Hummer's method. But even after the oxidation, the main structure of graphite will be retained and is validated by the peak at  $1600\text{ cm}^{-1}$ .

The ZnO frequencies obtained from the infrared studies are in accordance with literature values [16]. The inter-atomic vibrations in the metal-oxide nanoparticles give a fingerprint absorption region below  $1000\text{ cm}^{-1}$ . The water molecules adsorbed on Zn surface is verified with presence of peaks at  $3450\text{ cm}^{-1}$  and  $1090\text{ cm}^{-1}$ . The peaks at  $1640\text{ cm}^{-1}$  and  $450\text{ cm}^{-1}$  are the stretching and deformation vibrations respectively. FTIR spectrum ascertains the purity of the nanoparticles.

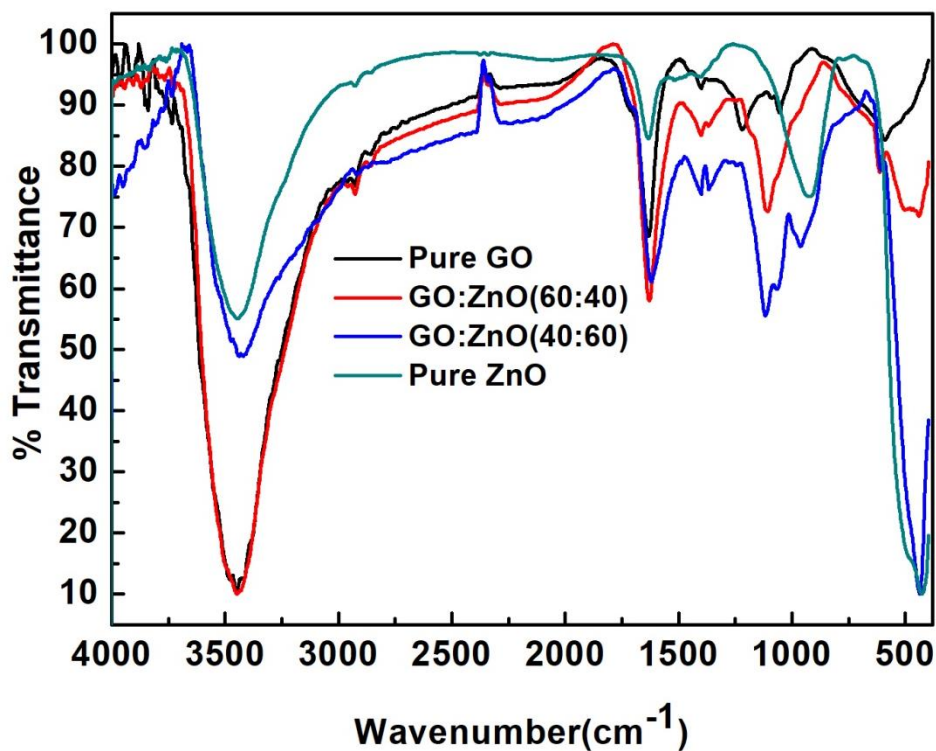


**Figure 2.** FTIR analysis of GO-ZnO composite at various concentration

In the case of GO-ZnO composite, there is a substantial reduction of GO and it in turn reduced the oxygen functional groups in the composite milieu [17]. The absorbance peak at  $1600\text{ cm}^{-1}$  and  $450\text{ cm}^{-1}$  signifies the skeletal vibration of graphene sheets ( $\text{C}=\text{C}$ ) and stretching vibration of ZnO. Thus, these evidences signify the alignment of ZnO on GO matrix. The O-H stretch corresponding to the hydroxyl group was observed at  $3400\text{ cm}^{-1}$ . The peak at  $1060\text{ cm}^{-1}$  was attributed to the presence of carbonyl group in the ZnO-GO structure.

### 3.2. Optical characterization

The optical properties of the GO-ZnO nanocomposite were elucidated with UV-Vis spectroscopy. The UV spectrum of GO-ZnO nanocomposite along with the pure GO and ZnO is presented in Fig 3. The spectrum exhibits diminutive absorption in the visible and infrared region but elevated absorption in the UV region.

The  $n-\pi^*$  transitions in the aromatic C-C bond of GO attribute to the absorption at 237 nm [18]. Wherein, ZnO a broad absorption peak is found to be around 371 nm which is trait of the wurtzite hexagonal phase ZnO, indicating that the synthesized product is a pure ZnO [19]. The intensity of this peak decreases with the increase in the concentration of GO.

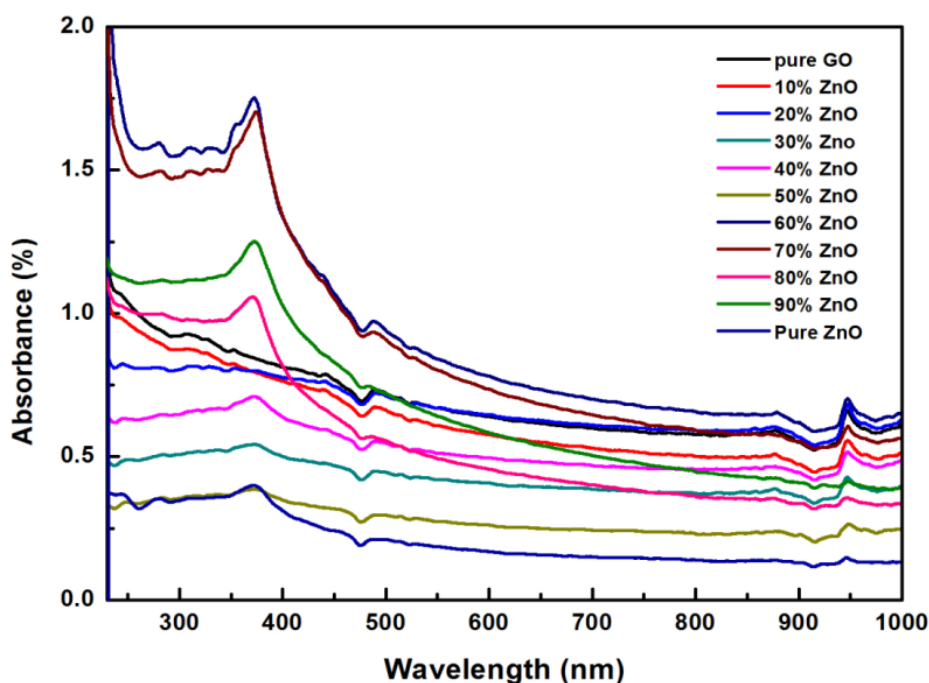


**Figure 3.** UV absorption spectra of GO-ZnO composite at various concentration

The energy gap of the pure sample and the composites are estimated using Tauc plot and given in Table 1. The band gap of the GO was found to be 5.086 eV while that of ZnO was estimated to be 3.072 eV. The energy band gap of all the composites is seen to be decreased with the increase in quantity of ZnO. For composite higher concentration of ZnO-GO, there are two transitions owing to the band gap of both GO and ZnO.

**Table 1.** Energy Band gap of GO-ZnO composite.

Wt % of ZnO in GO	Energy gap (eV)
Pure GO	5.086
10%	4.939

20%	4.889
30%	4.771
40%	4.704
50%	4.760
60%	4.480
70%	4.408
80%	4.401
90%	4.369
Pure ZnO	3.072

### 3.3. Impedance analysis

The trend of variation of electrical parameters of composite over a frequency range 20Hz – 1MHz was studied and the same is depicted in figure 4.

The composite exhibits high resistance and capacitance at low frequency in room temperature. The resistance increased manifold with concentration of GO in the composite. Whereas, the resistance sharply declines as the frequency increases to 1 MHz. The capacitance value is very high for 60%, 50% and 20% of ZnO in GO-ZnO composite.

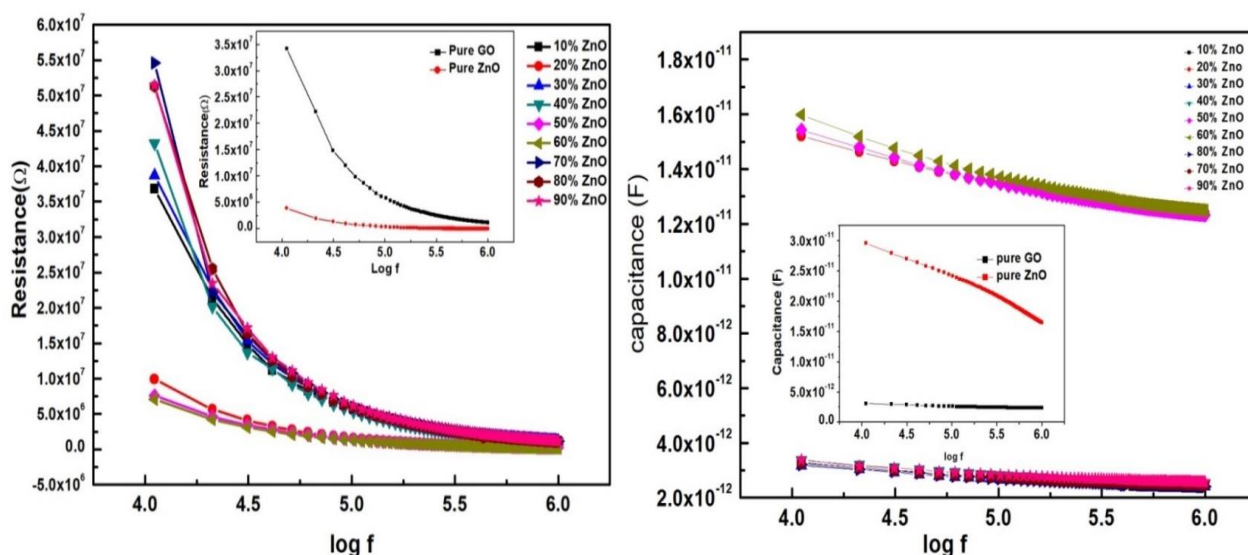


**Figure 4.** Variation of resistance and capacitance as function of frequency for GO-ZnO nanocomposite.

The frequency dependent ac electrical conductivity of all the GO-ZnO nanocomposites is illustrated in Fig 5. The dependence of ac conductivity on frequency is due to the interface charge polarization and intrinsic electric dipole polarization. The increase in AC conductivity in an ionic solid with an applied frequency is the contribution of the driving force of the field in migrating charge carriers between different localized centers as well as releases the raptions from trapped states. These

charge carriers along with the electrons from the valence exchange of metal ions augment the conduction process. That is, the augmented conductivity on applied frequency is primarily due to the enhanced mobility of charge carriers as a result of the increase in frequency at which electron hops [19-22]. At lower frequencies, the declination in the number of mobile ions can be attributed to the impedance of charge carriers by electrode interface and hence low conductivity. Frequency independent behaviour of conductivity in low frequency region is also observed. But also it is observed for the composite below 50% ZnO in GO, the conductivity is independent of frequency and shows a plateau. The conductivity was found to decrease drastically with high GO content in the composite. The maximum conductivity was for those composites with greater than 50% of ZnO and for the composite below 50% ZnO in GO, the conductivity is independent of frequency and shows a plateau.

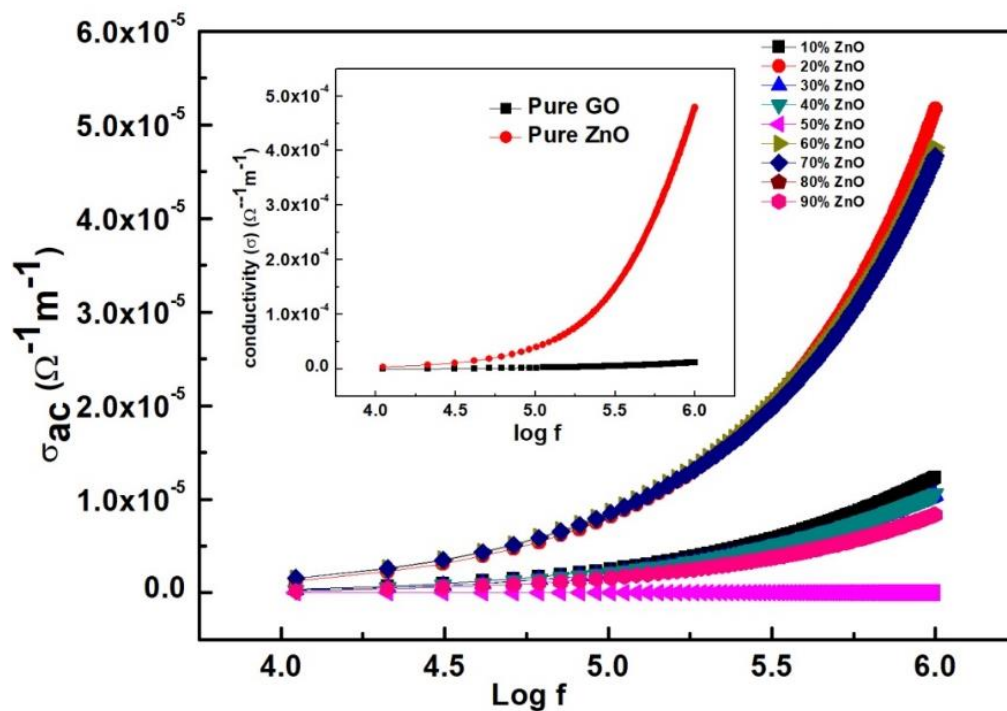


**Figure 5.** Conductivity ( $\sigma_{ac}$ ) as a function of frequency (For various concentration of GO-ZnO composite)

The decrement in dielectric constant with increase in frequency is a consequence of the scattering of charge carriers and the rapid deviation of electric field. This general trend for any dielectric material and the similar behaviour is shown by GO-ZnO composites (fig.6)

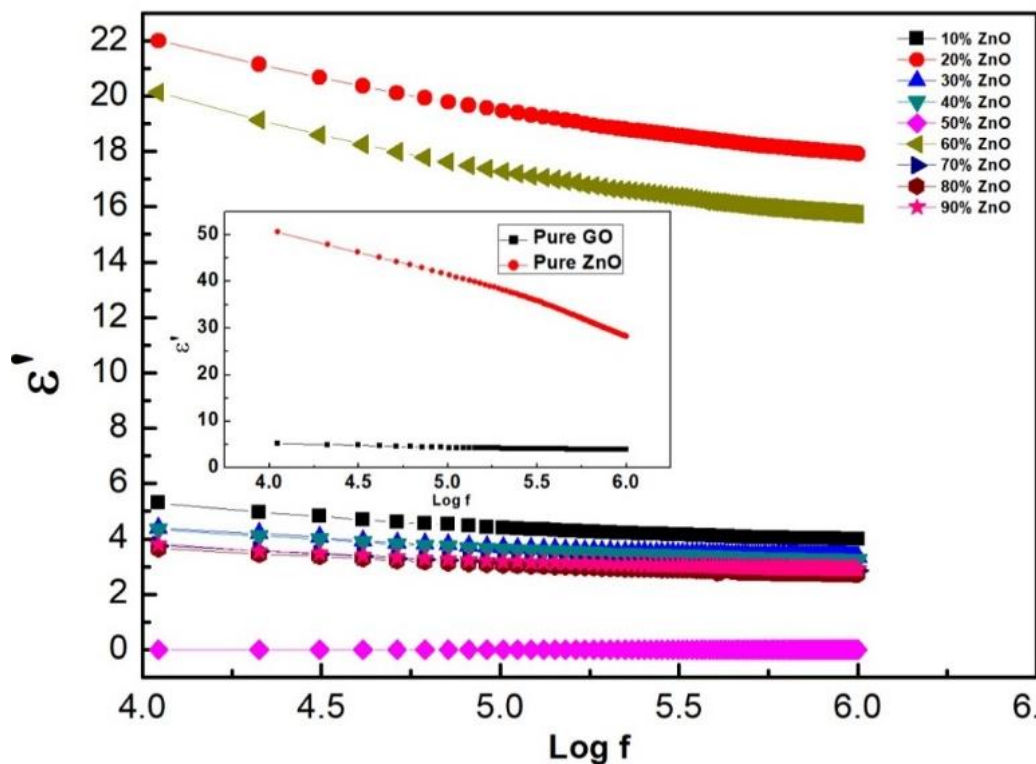


**Figure 6.** Real dielectric constant as a function of frequency (For various concentration of GO-ZnO composite)

The dielectric analysis measures two elementary electrical traits of materials such as, the ability to store and transfer the electronic charge. At lower frequencies,  $\epsilon'$  for polar materials is given by the sum of all the polarizability components which include ionic, electronic, orientation and interface polarization. The displacement of the valence electrons and positive nucleus with respect each other endorse electronic polarization ( $10^{16}$  Hz) whereas, ionic polarization ( $10^{13}$  Hz) arises due to the displacement of negative ions relative to positive ions. In case of Dipolar polarization ( $10^{10}$  Hz), it is the contribution from the change in orientation of permanent electric dipole moment with the direction of applied field. It takes place around the frequency of about. The last is the space charge polarization (1 to  $10^3$  Hz) which occurs due to accumulation of carriers at interfaces. These contribute from all the components is prominent in a dielectric material. Since the time consumption by the dipoles to orient themselves under a high frequency is more, this decreases the value of the dielectric constant  $\epsilon'$  and finally attains a constant value. It is noticed that the GO-ZnO composite with 20% and 60% of ZnO shows the highest dielectric constant which is in the range of that of a semiconductor [21-23].

The variation of ( $\epsilon''$ ) with frequency is shown in figure 7. At lower frequencies, it is the dipole polarization contributes to the increase of imaginary part of the dielectric constant, i.e. dipole loss. And  $\epsilon''$  at moderate frequencies is characterized by the conduction loss of ion migration along with ion polarization. At high frequencies vibration losses are the main source, so  $\epsilon''$  decreases. Similarly the presence of ZnO enhanced the imaginary part of the dielectric constant in GO-ZnO composite at 20% and 60% ratios of ZnO in GO-ZnO composite.



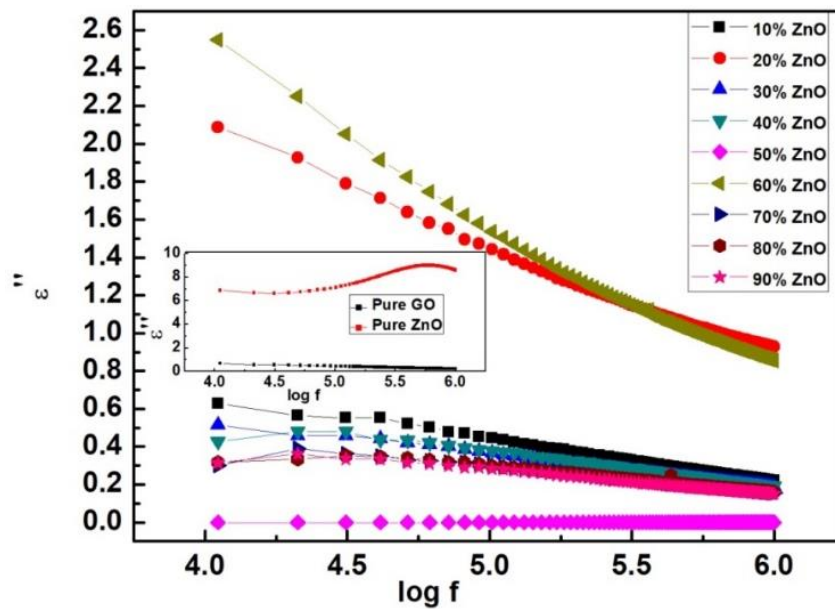


**Figure 7.** Imaginary dielectric constant as a function of frequency (For various concentration of GO-ZnO composite)

The dielectric loss,  $\tan\delta$  ( $\tan\delta = \frac{\epsilon''}{\epsilon'}$ ), as a function of frequency, for GO-ZnO composite together with the pure GO and ZnO (insert) is presented in Fig.8.

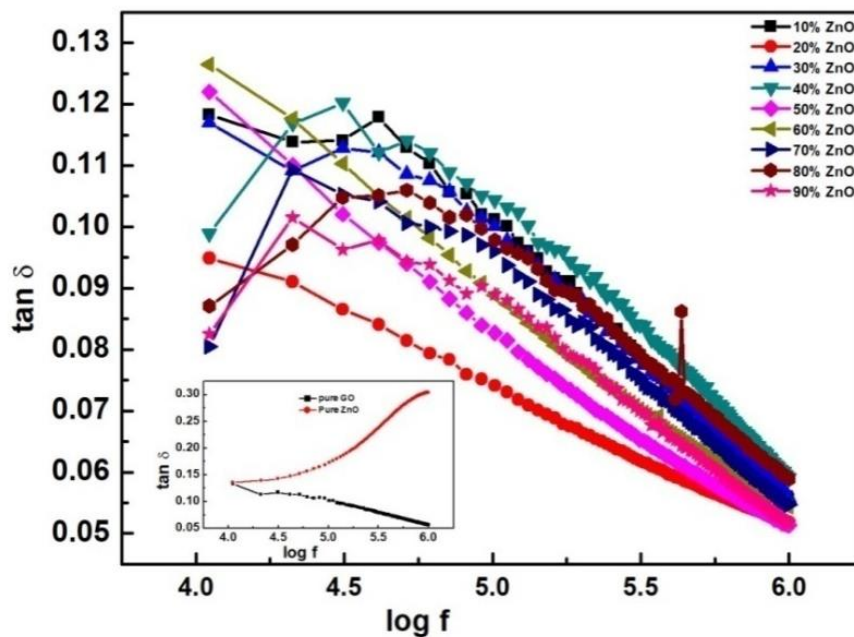


**Figure 8.** Variation of dielectric loss ( $\tan\delta$ ) as a function of frequency(For various concentration of GO-ZnO composite)

The dielectric loss represents the energy loss in the system. The loss tangent for pure ZnO increases with the frequency and has a very high value at high frequencies, while that of pure GO show a decrease with frequency attaining low values at higher frequencies. A high dielectric loss at low frequency at all ratios of GO-ZnO Nano composite is observed. This may be ascribed to the high resistivity at low frequencies. Also the tangent loss for the composite shows very much low value compared to that of pure ZnO implying that these composites are very much suitable for electronic applications such as fabrication of capacitors [24-25].

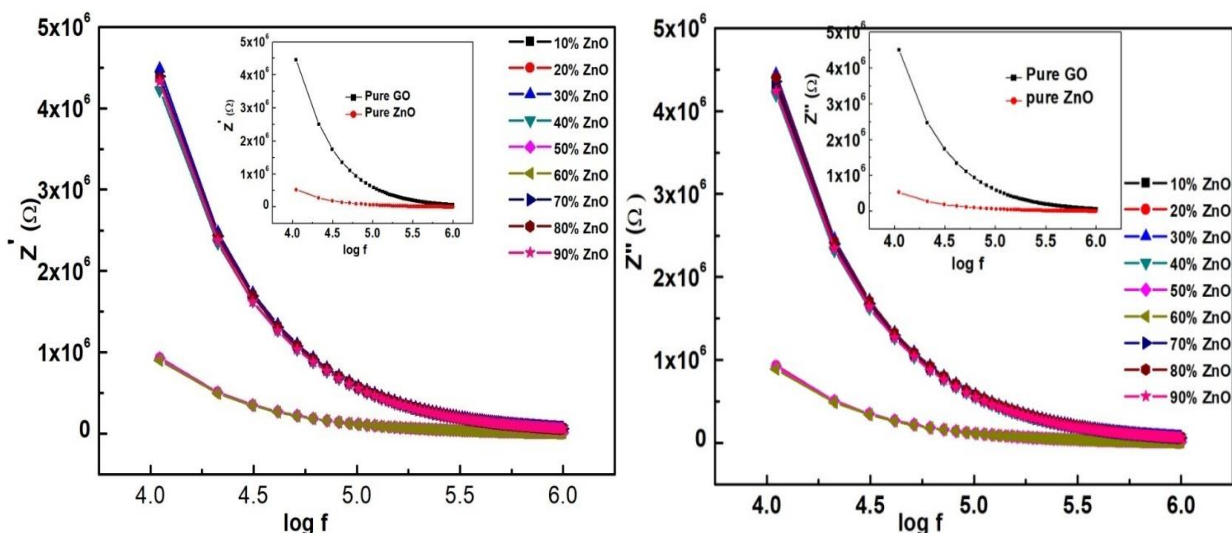


**Figure 9.** (a) Real impedance as a function of frequency (b) imaginary part of impedance variation with frequency (For various concentration of GO-ZnO composite)

The trends of variation of  $\epsilon'$  and  $\epsilon''$  with frequency for the different ratios concentration of GO-ZnO Nano composite and the pure compounds are shown in Fig.9 (a&b). The decrement in the values of  $Z'$  and  $Z''$  is because of the space charge polarization. Higher values of impedance at low frequency, implies that the polarization is larger [26-27]. The frequency independent behaviour at higher frequency is suitable for high frequency device applications. For the ratios of 20% and 60% of ZnO in GO, we see a significantly low impedance. This indicates an improved conductivity of GO-ZnO nanocomposite at these ratios due to the introduction of ZnO in GO.

#### 4. CONCLUSIONS

In present study ZnO nanoparticles and GO are synthesized by implementing precipitation method and hummer's method respectively. The structural composition of ZnO, GO and the composites have been investigated. From the XRD results the size of ZnO nanoparticles were estimated as 15nm and that of GO 6nm. The inter planner distance of GO was found to be 0.78 nm, a clear indication of the oxidation of GO. The energy band gap of all the composites is seen to decrease with the increase of

the quantity of ZnO. It is observed that the AC conductivity ( $\sigma_{ac}$ ) gradually increases with an increase in frequency and is attributed to the interface polarization and intrinsic dipole polarization. It is noticed that the GO-ZnO composite with 20% and 60% of ZnO has the highest dielectric constant which is in the range of that of a semiconductor. The decrease of imaginary part of the dielectric constant with frequency is attributed to the migration of ions. Similarly the presence of ZnO enhanced the imaginary part of the dielectric constant in GO-ZnO composite with the best results been obtained at 20% and 60% ratios of ZnO in GO-ZnO composite. The loss tangent for pure ZnO increases with the frequency and has a very high value at high frequencies, while that of pure GO show a decrease with frequency attaining low values at higher frequencies. Also the tangent loss exhibit very low value for the composite compared to pure ZnO. These composites are promising for electronic applications such as fabrication of super capacitors and batteries.

## References

1. B. Manoj, M.R. Ashlin and T.C. George, *Scientific reports*, 7(2017)18012.
2. Li, Ping, Bin Lu and L. Zhanzhou, *Bulletin of Materials Science*, 40(2017)1069.
3. J. Wu, X. Shen, L. Jiang and K. Chen, *Applied surface science*, 256 (2009)2826.
4. T. Riya, E. Jayaseeli, N.S. Sharma and B. Manoj, *Results in Physics*, 10(2018)633.
5. A.G. Kunjomana and B. Manoj, *Asian Journal of Materials Science*, 2(2010)204.
6. S.R. Brintha and M. Ajith, *IOSR Journal of Applied Chemistry*, 8(2015)66.
7. B. Manoj, M.R. Ashlin and T.C. George, *Scientific reports*, 8(2018)13891.
8. A.G. Kunjomana and B. Manoj, *Russian Journal of Applied Chemistry*, 87(2014)1726.
9. M. Pandey, G. M. Joshi, A. Mukherjee, and P.Thomas, *Polymer International*, 65(2016)1098.
10. B. Manoj, *Research Journal of Biotechnology*, 8(2013)49.
11. B. Manoj, *Journal of Environmental Research and Development*, 9(2016) 209.
12. C.D. Elcey and B. Manoj, *Research Journal of Chemistry and Environment*, 17(2013)11.
13. Saranya, Murugan, R. Rajendran and W. Fei, *Journal of Science: Advanced Materials and Devices* 1(2016)454.
14. B. Manoj, *Russian Journal of Physical Chemistry A*, 89(2015)2438.
15. B. Manoj, *International Journal of Coal Science & Technology*, 3(2016)123.
16. E. Salih, M. Mekawy, R. Y. Hassan and I. M. El-Sherbiny, *Journal of Nanostructure in Chemistry*, 6(2016)137.
17. B. Manoj, M.R. Ashlin and T.C. George, *Materials Science-Poland*, 36(2018)14.
18. M. Khan, J. Pooja and B. Manoj, *Asian Journal of Chemistry*, 30(2018).
19. N. Preda, M. Enculescu, C. Florica, A. Costas, A. Evangelidis, E. Matei and I. Enculescu, *Digest Journal of Nanomaterials and Biostructures*, 8(2013)1591.
20. I. Latif, T. B. Alwan and A. H. Al-Dujaili, *Nanoscience and Nanotechnology*, 2(2012)190.
21. B.P. Prasanna, D. N. Avadhani and H. B. Muralidhara, *International Journal of Latest. Technology in Engineering. Management and Applied Science*, 3(2014)55.
22. D. Wang, X. Zhang, J.W. Zha, J. Zhao, Z.M. Dang and G.H.Hu, *Polymer*, 54(2013)1916.
23. R.Vargas, K.P. Ludmila, L.D. Anne, Rita de Cássia, C.B.de Souza, M.R. Baldan and S.G. Emerson, *Journal of Aerospace Technology and Management*, 9 (2017)29.
24. N. Shukla and D. K. Dwivedi, *Journal of Asian Ceramic Societies*, 4(2016)178.
25. A. R.Polu, R.Kumar, V. Causin and R.Neppalli, *Journal of Korean Physical Society*, 59(201)114.

26. G. Kumar, J.Shah, R.K. Kotnala, P. Dhiman, R. Rani, V.P. Singh, G. Garg, S.E. Shirsath, K.M. Battoo and M.Singh, *Ceramics International*, 40(2014)14509.
27. S. Kazmi, H.Salman and A. Ameer , *India Conference (INDICON),Annual IEEE*, 2015.

© 2019 The Authors. Published by ESG ([www.electrochemsci.org](http://www.electrochemsci.org)). This article is an open access article distributed under the terms and conditions of the Creative Commons Attribution license (<http://creativecommons.org/licenses/by/4.0/>).